



# Accelerator-based neutron source for boron neutron capture therapy

Yoshiaki Kiyanagi

Graduate School of Engineering, Nagoya University, Furo cho, Chikusa ku, Nagoya, Aichi 464-8603, Japan

Correspondence to: Yoshiaki Kiyanagi. Graduate School of Engineering, Nagoya University, Furo cho, Chikusa ku, Nagoya, Aichi 464-8603, Japan.

Email: kiyanagi@phi.phys.nagoya-u.ac.jp.

**Abstract:** A beam shaping assembly (BSA), a neutron moderator system, is a key component of an accelerator based boron neutron capture therapy (BNCT) facility. The neutron energy recommended in the IAEA TECDOC-1223 for the BNCT is much lower than the energy of the neutrons produced by accelerator induced nuclear reactions. The neutron energy depends on the energy of the incident particle and nuclear reaction. Therefore, the BSA should be designed considering the neutron energy dependency. Now, several kinds of accelerators and reactions are used and proposed. Here, neutron producing reaction, moderator system, and activations are introduced.

**Keywords:** Boron neutron capture therapy (BNCT); neutron source; target; moderator; proton energy

Received: 27 August 2018; Accepted: 18 October 2018; Published: 23 November 2018.

doi: 10.21037/tro.2018.10.05

View this article at: <http://dx.doi.org/10.21037/tro.2018.10.05>

## Introduction

Boron neutron capture therapy uses  $\alpha$  and Li particles produced by a neutron induced nuclear reaction with a boron nucleus to kill cancer cells. Therefore, high intensity neutron sources are desired for highly efficient treatment. Nuclear reactor neutron sources have been used for boron neutron capture therapy (BNCT) for a long time since high intensity neutron beams have been supplied only by reactors (1). Furthermore, many of the reactors have been shut down and then the number of reactors for BNCT reduced. Only one reactor constructed recently for BNCT is in China (2). On the other hand, accelerator-based neutron sources are becoming popular in neutron application fields (3). However, neutron intensity for BNCT is rather high compared with that produced by a conventional accelerator with a power of few kW. A high intensity neutron source more than  $10^{13}$  n/sec at a neutron generation target is required and there was no accelerator that could apply to BNCT. Demand to construct a BNCT facility in a hospital has been very high, and at last, BNCT facilities using proton accelerators with a power of few 10 kW have been developed (4,5), and also constructed in the hospitals in Japan (6-8).

So far, protons are used for neutron production, and their energies range from 1.45 MeV to 30 MeV. An electron accelerator was studied for BNCT (9) but not yet realized. For low energy protons, a Li neutron target is used and a Be target is used around 10 MeV or more. Blistering caused by protons is one of big issues for target design. Neutron yield per proton becomes higher with increasing the proton energy. However, the neutron energy also becomes higher and high energy neutrons need more process than lower energy ones to get to the energy suitable for the BNCT. Therefore, choice of a neutron moderator suitable for each system is important. IAEA TECDOC-1223 (10) indicates a guide line to BNCT for brain cancer to use epithermal neutrons, although for cancers at shallow place such as a skin cancer, and a head and neck cancer, a different guide line is required for the use of thermal neutrons. However, the guide line using the epithermal neutrons is the only one guideline now existing, and the neutron sources to produce the thermal neutrons are rather easy to design compared with the epithermal neutron source. Therefore, design study of neutron sources here is introduced mainly based on the IAEA TECDOC-1223.

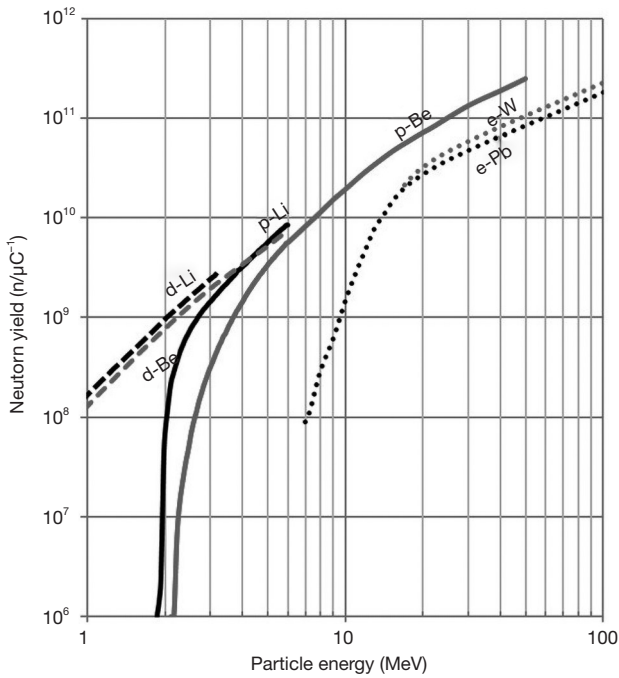
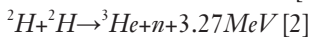
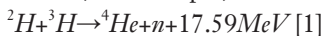


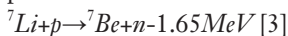
**Figure 1** Neutron yields of various reactions as a function of projectile energy. This data was created by partially using the data in Ref. (11).

### Neutron production reactions

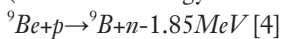
For neutron production, various nuclear reactions have been used, for example, fusion reactions of



proton reactions of

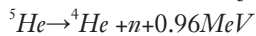
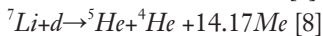
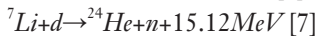
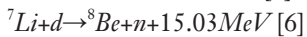
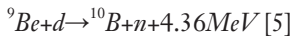


(Threshold energy =1.88 MeV)



(Threshold energy =2.06 MeV),

and deuteron reactions of



Neutron production by an electron accelerator that uses (e,X) and (X,n) reactions (photonuclear reaction) in a heavy metal target is another candidate. *Figure 1* shows neutron intensity as a function of the projectile energy (11). It is recognized that at low energy region d-Be and d-Li are effective, and then p-Li and p-Be. At an energy range above

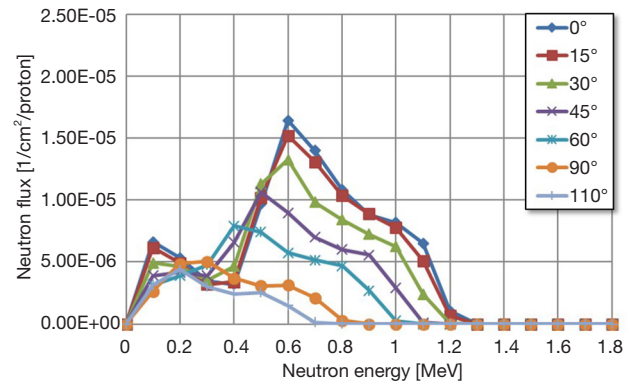


**Figure 2** Neutron energy spectra at various emission angles for the p-Li reaction at a proton energy of 2.8 MeV.

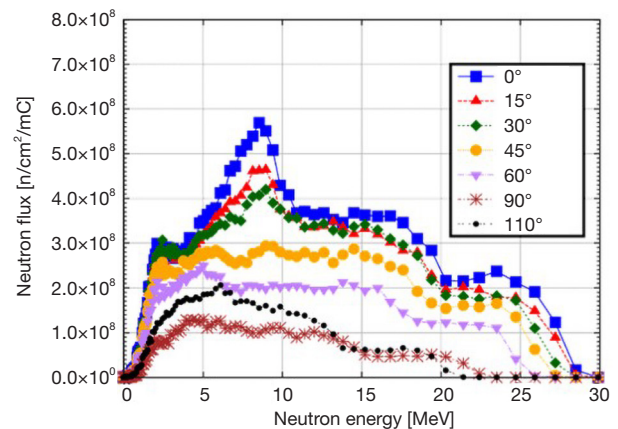


**Figure 3** Neutron energy spectra at various emission angles for the p-Be reaction at a proton energy of 30 MeV.

around 10 MeV p-Be has better performance. The fusion reactions have not been used as BNCT neutron sources, since their neutron yields are not enough for the treatment. The deuteron reactions are candidates for the low energy accelerators (12) and under development. The photonuclear reaction by the electron accelerator produces high intensity X-rays and the X-rays contaminate the irradiation neutron beam. This is one of problems to overcome when using the electron accelerator.

At present, the p-Be neutron sources were constructed in the hospital BNCT, Southern Tohoku Hospital (6) and Osaka Medical College (7), and the p-Li source in National Cancer Center (8). Therefore, here, the neutron sources based on p-Be and p-Li reactions are described. *Figure 2* shows an energy spectrum obtained by the p-Li reaction at 2.8 MeV, and *Figure 3* shows that obtained by the p-Be

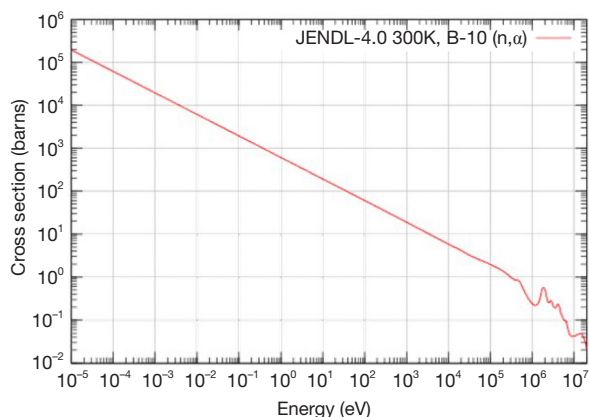


Figure 4 Neutron capture cross section of  $^{10}\text{B}(n,\alpha)^7\text{Li}$  reaction.

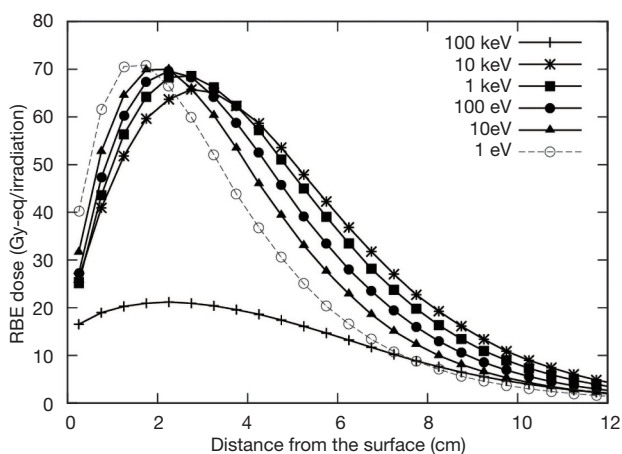


Figure 5 Dose distributions in a water phantom when monoenergetic neutrons injected (16).

reaction at 30 MeV. The p-Li distribution was calculated by using the Li-Yield (13), and the p-Be by MCNPX (14). The energy produced by the p-Li is much lower than that by the p-Be. Therefore, efficiency to slow down to the suitable neutron energy range for BNCT is better in the p-Li case than p-Be one.

### Design philosophy of the neutron source

Now, the BNCT treatment has been applied to various cancers, such as brain cancer, head and neck cancer, skin cancer. Figure 4 shows the neutron cross section for (n,α) reaction of boron (15). The absorption cross section is inversely proportional to the neutron speed or  $E^{1/2}$ . Therefore, high intensity neutrons having low energy are required at

Table 1 Recommended beam characteristics in IAEA TEC-DOC-1223

Beam characteristics	Recommended value
Epithermal neutron flux	$\geq 1 \times 10^9 \text{ n/cm}^2/\text{s}$
Fast neutron component	$\leq 2 \times 10^{-13} \text{ Gy}\cdot\text{cm}^2$
γ-ray component	$\leq 2 \times 10^{-13} \text{ Gy}\cdot\text{cm}^2$
Thermal neutron ratio	$\leq 0.05 \text{ s}$
Current/flux ratio	$\geq 0.7$

the cancer position to induce the neutron capture by boron, which produce α and Li particles. In the human body which major component is water, neutrons form an energy spectrum almost come to equilibrium with temperature of the medium. Therefore, the energy peak of the spectrum appears around the energy of ambient temperature, ~300K or 0.0253 eV. We call the neutron around this energy as thermal energy neutron or thermal neutron. If neutrons with an energy higher than thermal energy enter the human body they move in the human body before getting to the thermal equilibrium. Therefore, in general, higher energy neutrons give higher thermal neutron flux at a deep place of the human body. However, at an energy range over few 10 keV the effect decreases due to the neutron slowing down efficiency. Figure 5 shows dose distributions in a water phantom for tumor with boron when monoenergetic neutrons are injected into the phantom (16). The peak position shifts towards the deep position in the phantom but the peak dose decreases. Furthermore, the high energy neutron relatively increases neutron dose at skin, since it has high Kerma factor. Therefore, to use the high energy neutrons are not preferable even if they can get to a deep region. Nevertheless, since treatment at deep position is desired, a neutron energy range of epithermal neutrons (from 0.5 eV to 10 keV) was recommended in IAEA TECDOC-1223, and a flux value of  $10^9 \text{ n/cm}^2/\text{sec}$  was also. Furthermore, recommended values for components such as fast neutron component, γ-ray component, thermal neutron ratio and current-flux ratio (relating to beam divergence) in a neutron beam were indicated. The values are summarized in Table 1.

Here, the neutron source design to produce the epithermal neutrons is described.

### Neutron moderation system

#### Neutron target

The beam shaping assembly (BSA), namely a neutron

moderator system, consists of a target, a moderator, a filter and a reflector. The target is one of difficult parts to design at few 10 kw accelerator powers. Be and Li are used as the target materials at present. The Be target is used, in general, over about 5 MeV proton energies, and the Li target is used less than about 3 MeV. For the target design, blistering and radioactivity are important components to be considered as well as cooling. The target structure changes depending on the proton energy. *Figure 6* shows a calculation result of heat deposition in a Be target at various proton energies

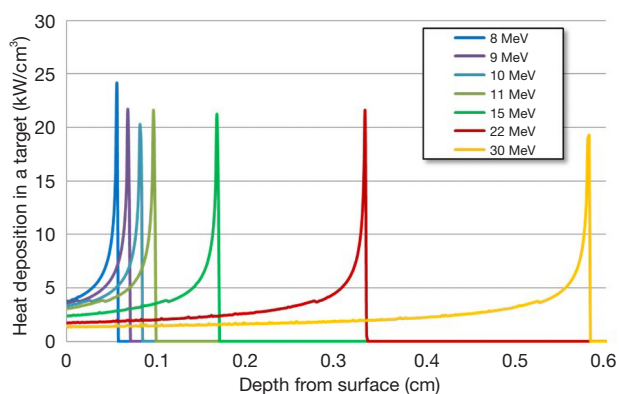


Figure 6 Heat deposition in a Be target at various proton energies.

with the use of MCNPX (14). As well known, a Bragg peak appears at the end of the proton trajectory. The proton energy around the Bragg peak is less than the threshold energy for the neutron production. Therefore, usually we can avoid appearing the Bragg peak in the target without serious reduction of neutron intensity since it will cause the highest heat deposition and the blistering in the target, and then shorten the target life.

As seen from *Figure 6* the target thickness is about several mm at a high energy proton about 30 MeV. In this case we can use the Be target as a part of structure materials since it has enough thickness, and the protons enter cooling water behind the target as shown in *Figure 7A*. This is a method to make a stable Be target (4). On the other hand, at lower proton energy another method to mitigate the blistering has to be adopted as shown in *Figure 7B*. The blistering for various materials were studied by using protons (17). A comparison of the blistering limits of Cu between 100 and 200 keV protons was performed and gave data that the blistering limit of 200 keV proton is much higher than the 100 keV case. A Cu block with cooling channels is usually used for the target cooling. Materials with high hydrogen diffusion constant would be candidate materials to mitigate the blistering. Properties of such materials, V, Nb, Ta and Pd are summarized in *Table 2* (17,22) as well as Cu data.

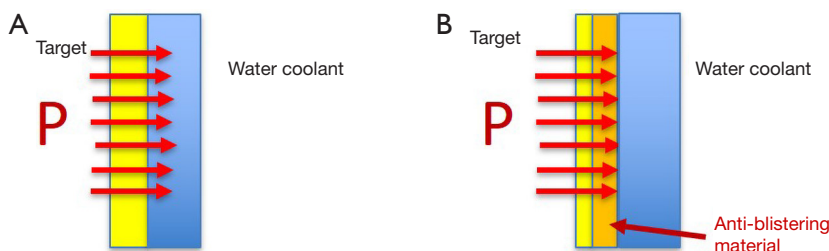
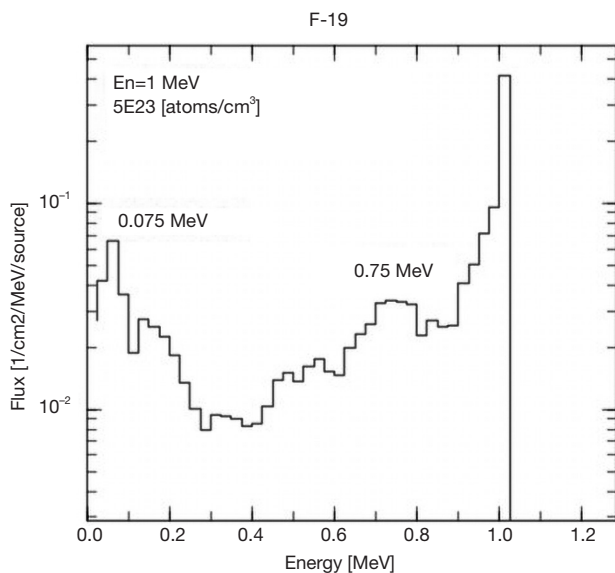


Figure 7 Schematic view of a target design around 30 MeV proton (A) and that for low energy proton (B).

Table 2 Characteristics of anti-blistering material

Variables	V	Nb	Ta	Pd	Cu
Blistering limit ( $10^{22}/m^2$ )	Not observed up to 120 (17)		Not observed up to 230 (17)	200–300 (17)	0.04–0.1 (17)
Hydrogen diffusion coefficient ( $m^2/s$ ) at 25 °C	$5 \times 10^{-9}$ (18)	$8 \times 10^{-10}$ (19)	$2 \times 10^{-10}$ (20)	$4 \times 10^{-11}$ (21)	$2 \times 10^{-14}$ (21)
Thermal conductivity (W/m/K)	30.7	53.7	57.5	71.8	401
Melting point (°C)	1,910	2,477	3,017	1,555	1,084
Major activation product (half-life)	$^{52}V$ (3.7 m) (22)	$^{93m}Nb$ (16.1 y) (22)	$^{182}Ta$ (114 d)	$^{103m}Rh$ (56 m) (22)	$^{64}Cu$ (12.7 h) (22)



**Figure 8** Transmission spectrum of 1 MeV neutrons through a F plate.

The table also includes radioactive product of each material. The blistering characteristics for Cu were also investigated by using 750 keV protons (23). All data indicated that Cu has low value of the blistering limit. Therefore, the protons should not be injected into Cu since it will shorten the life time of the target. There were no data about Nb in Ref. (17). However, other data existed, and the limit value was about 4 times lower than that of V (23-25). To make a long-life target, a material with high tolerance to the blistering is placed behind the target as shown in *Figure 7B*. One example is for a proton linac with an energy of 7 MeV and a current of 0.1 mA for the neutron science use (22). They chose V as the anti-blistering material, which activity after the irradiation is high but decays quickly. The other is for a proton linac with an energy of 8 MeV and a current of 5 mA for BNCT (5). They examined bonding of a three-layered structure, Be, anti-blistering material and Cu. As intermediate materials, Pd, Nb, Ta, and Ti were tried to be bonded by using a hot isostatic pressing method (26). For Li target, two methods were proposed. A liquid Li target is one candidate. For that a liquid Li loop is constructed to make thin Li layer as a neutron production place (27,28). However, this system is under development. On the other hand, a solid Li target was already used and animal tests were performed (29). A new system has been proposed (30,31). In such a solid target, anti-blistering material such as Pd was used just behind the Li layer.

About the radioactivity point view, the Be reaction does not produce radioactive elements less than about 10 MeV, but the Li reaction produce  $^7\text{Be}$  and its half-life is 53.5 days. A special method to handle the target is required.

### Moderator

Design of a BSA depends on the proton energy since the produced neutron energy spectra changes since the maximum neutron energy is expressed approximately by (proton energy – threshold energy). The neutron energy is much higher than the recommended neutron energy for BNCT. Therefore, we need neutron moderator. One of major processes of the neutron moderation is elastic scattering of moderator nucleus. Ratio of the scattered neutron energy  $E_2$  to the initial energy  $E_1$  is expressed by the next formula.

$$E_2/E_1 = [(1+\alpha) + (1-\alpha)\cos\theta]/2 \quad [9]$$

Here,

$$\alpha = [(A-1)/(A+1)]^2 \quad [10]$$

$A = M_a/M_n$  ( $M_a$  and  $M_n$  are masses of moderator nucleus and neutron), and  $\theta$  is scattering angle in the center of mass system. Therefore, lighter nucleus is better for slowing-down. For obtaining thermal neutrons that is effective for cancer at shallow position, hydrogen and deuterium containing materials are optimal since they have high slowing-down efficiency and a thermal equilibrium spectrum at ambient temperature is obtained. Deuterium containing material such as heavy water is better than light water since it does not produce  $2^{\text{nd}}$   $\gamma$ -rays emitted by neutron absorption. However, according to the IAEA TECDOC-1223, neutrons from 0.5 eV to 10 keV are desired for the deep position cancer. The neutron moderator effective to slow down to this energy range is different from hydrogenous materials. Little bit higher mass number nucleus than hydrogen are preferable. In such materials fluorine is the best candidate since it also has low threshold energy, about 100 keV, of inelastic scattering, another process of slowing-down, which can effectively reduce the neutron energy. *Figure 8* shows a transmitted neutron spectrum through a fluorine virtual plate by a simulation calculation using PHITS code (32) with JENDL-4.0 (15). The incident neutron energy was 1 MeV and this shows an example of the slowing-down scheme that indicates the effect of the inelastic scattering.

There are several materials including fluorine such as  $\text{MgF}_2$ ,  $\text{CaF}_2$ ,  $\text{PbF}_2$ , PTFE  $[(\text{CF}_2)_n]$  and Flual (AlF<sub>3</sub>: 69%, Al: 30%, LiF: 1%). Energy spectra were calculated at an

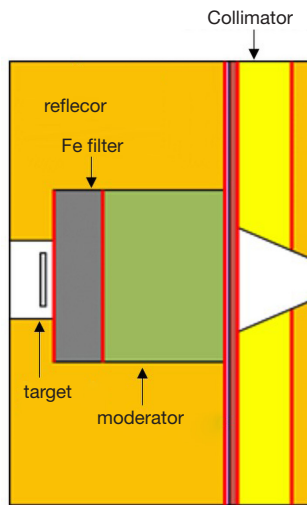


**Figure 9** A model BSA used for calculation of the neutron spectra of various moderator materials (33). BSA, beam shaping assembly.

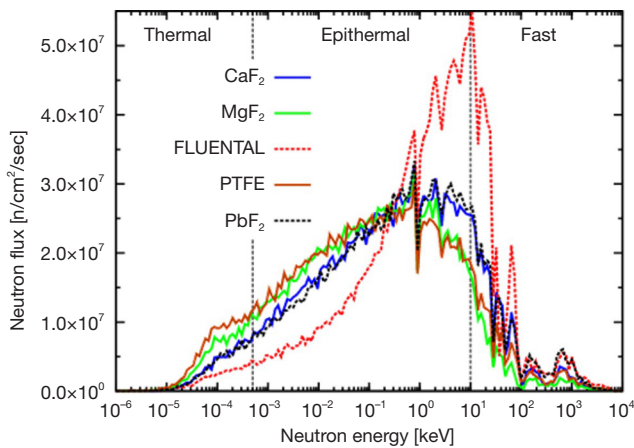


**Figure 10** Energy spectra at the exit of the collimator obtained by various moderator materials (33).

exit of a simple BSA shown in *Figure 9* (33). Here, an Fe-filter was placed between the target and the moderator, and Pb reflector was put around the target and the moderator. In this case, a proton energy of 8 MeV and a Be target were assumed. *Figure 10* shows the energy spectra obtained under the condition that the same epi-thermal neutron intensity was obtained in each moderator. The spectrum of Flualental has the highest fast neutron flux and the fast neutron component was also highest among the moderators studied here although the thermal neutron intensity was effectively reduced.  $PbF_2$  and  $CaF_2$  give almost the same spectrum but the flux of  $PbF_2$  moderator is little bit higher around

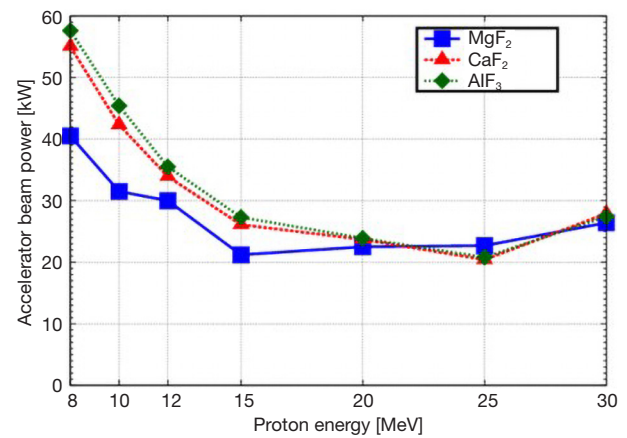


**Figure 11** Required accelerator beam powers for various moderator materials (34).

the peak.  $MgF_2$  and PTFE give almost the same spectrum but  $MgF_2$  is better than PTFE since PTFE gives higher fast and thermal neutron intensities.  $MgF_2$  gives the best performance among them and the difference among them is small other than Flualental.

Furthermore, it is considered that effectiveness of the moderator materials will depend on the proton energy or the produced neutron energy. Therefore, energy dependency was studied (34). Proton energies from 8 to 30 MeV were studied and required accelerator power was evaluated for moderator materials of  $CaF_2$ ,  $MgF_2$  and  $AlF_3$  under the condition of the same epithermal neutron intensity and fast neutron component. *Figure 11* shows the required accelerator powers for these materials. The required powers for these materials are almost the same at an energy region above around 15 MeV, and below this energy  $MgF_2$  is the best. Furthermore,  $MgF_2$  produce the same epithermal neutron intensity with minimum thickness of the moderator at every proton energy studied (34).

### Reflector

To obtain high intensity of the epithermal neutrons, the reflector should not have high slowing down efficiency. Therefore, high mass number materials are preferable due to Eq. [9] in moderator chapter. Pb, Bi, W and Fe can be considered as usually used materials. Pb and Fe would be realistic candidates since W is expensive and Bi produce  $\alpha$  emitter nucleus, Po, by absorption of neutrons. The neutron spectra emitted from the collimator exit were calculated by using a similar BSA shown in *Figure 9*. In this

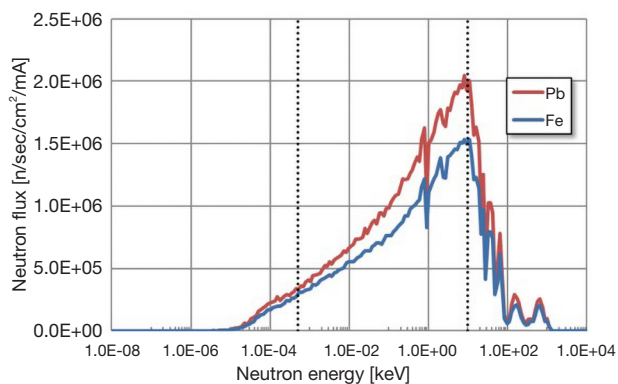


**Figure 12** Energy spectra at the exit of the collimator using Pb or Fe reflector.

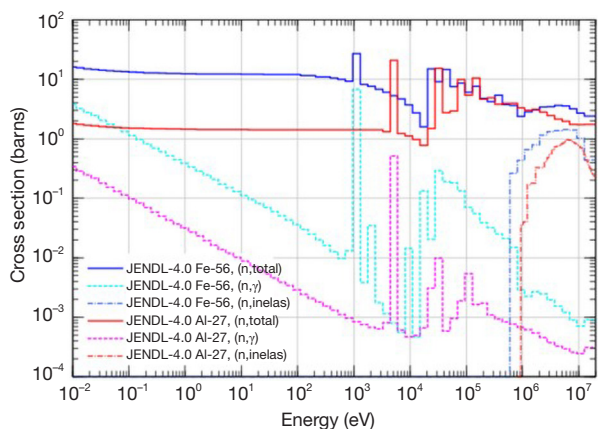


**Figure 13** Neutron cross section of Fe and Al.

case  $MgF_2$  was used as the moderator material. The energy spectra are shown in *Figure 12* and it was found that Pb gives higher intensity than Fe.

**Filter**

Filter is another issue to be studied. Fe and Al were studied since both have similar neutron cross section around MeV region as shown in *Figure 13* (15). The number densities of Al and Fe are  $0.0602 \times 10^{24}$  and  $0.0848 \times 10^{24}$  atoms/cm<sup>3</sup>, respectively. Al has lower cross section below about few 10 keV and over MeV. Both materials have a dip around 30 keV. Energy spectra at the exit of the collimator were calculated at proton energy 8 MeV using the same BSA shown in *Figure 9* (33). First, the Fe-filter BSA was designed to attain the epithermal neutron intensity of  $1.5 \times 10^9$  n/sec/cm<sup>2</sup>, little bit higher than the TECDOC

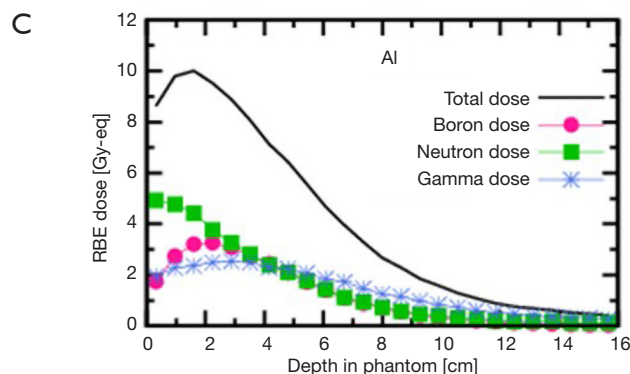
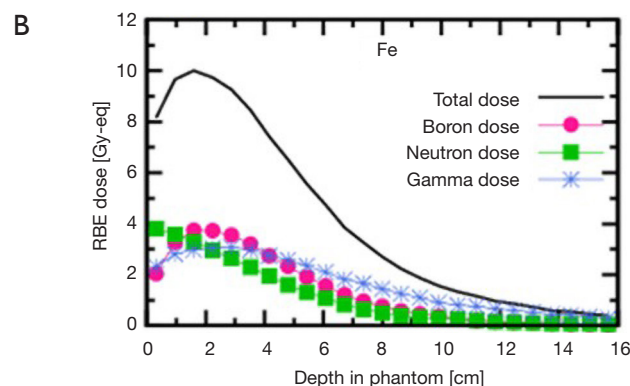
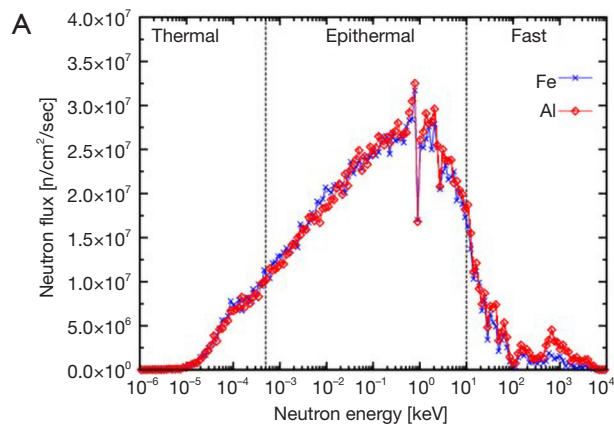


**Figure 14** Energy spectra (A) and dose distributions in a water phantom in the case of Fe (B) and Al (C) (33).

value, and then the Al-filter BSA was designed to attain the same epithermal neutron intensity. Therefore, the fast neutron component was different each other. The energy spectrum of the Al-filter BSA has almost the same shape in the thermal and epithermal region, but at high energy region the Al-filter BSA gives higher intensity as shown in *Figure 14A*. To check this effect, dose distributions in a water phantom were calculated under the condition on

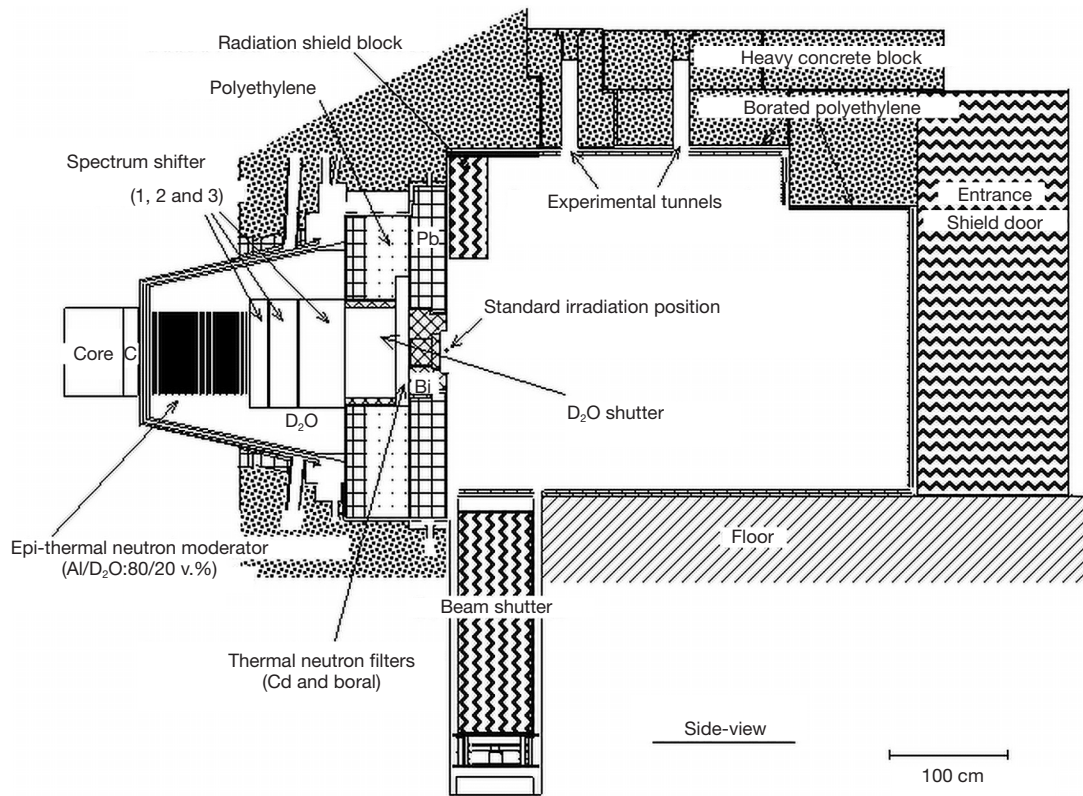


**Figure 15** Neutron moderation system and irradiation area of Kyoto University Reactor BNCT facility (35). BNCT, boron neutron capture therapy.

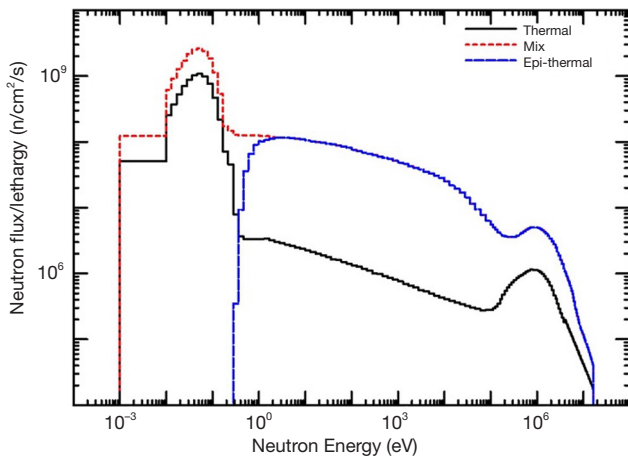


**Figure 16** Energy spectra obtained at Kyoto University Reactor BNCT facility (35). BNCT, boron neutron capture therapy.

10 ppm boron concentration in water. The result is shown in *Figure 14B,C*. In the case of the Al-filter, it is clearly recognized that neutron dose near the surface is much

higher than the Fe-filter case. However, the filter is not effective or reduces the epithermal neutron intensity at low energy proton less than about 3 MeV. Therefore, no filter was used for the p-Li neutron sources.

### Examples of existing facilities

Here, existing facilities are introduced. At first, the neutron source at Kyoto University Reactor, KUR (5 MW) is introduced as a reference to the accelerator-based facilities, since it has been used for BNCT for a long time and the number of the treatment is largest in the world (35). *Figure 15* shows the beam line of the KUR BNCT facility. It is equipped with an epithermal neutron moderator consisting of Al and D<sub>2</sub>O, and spectrum shifter of D<sub>2</sub>O. Various energy spectra are produced by using this moderator system. Typical energy spectra are shown in *Figure 16*, namely, thermal, mix and epithermal spectra.

The accelerator-based BNCT were constructed in Japan. Energies used are 30, 8 and 2.5 MeV, and the last one uses

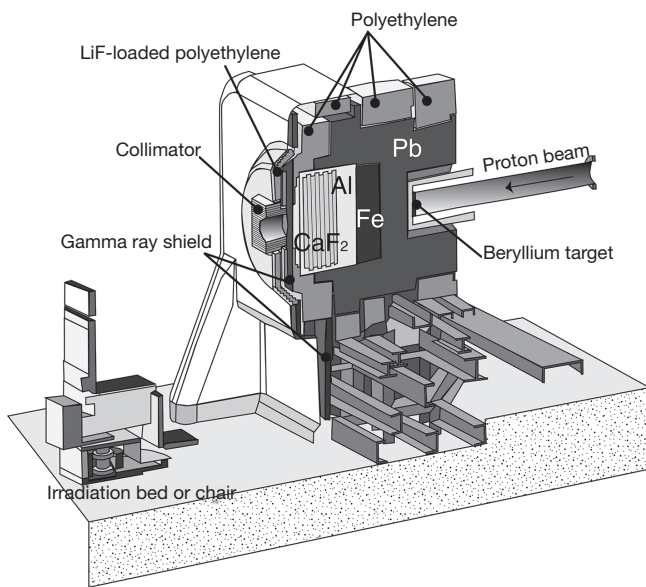


Figure 17 BSA of C-BENS (4). BSA, beam shaping assembly.

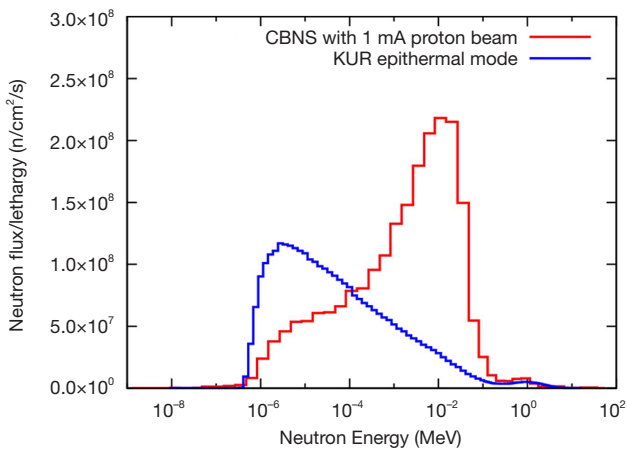


Figure 18 Energy spectra at C-BENS BSA and KUR (4). BSA, beam shaping assembly.

Li target. The first two were already presented (4,5). Here, these two facilities are introduced. The first facility in the world is C-BENS in Institute for Integrated Radiation and Nuclear Science, Kyoto University. Figure 17 shows the BSA of C-BENS. The proton energy and current are 30 MeV and 1 mA, and the produced neutron energy is less than about 28 MeV, very high. Therefore, to reduce the fast neutron component is one of the most important roles of the BSA. Here, Pb is used to produce neutrons by reactions such as (n,2n), and then Fe and Al are placed as filters. As a

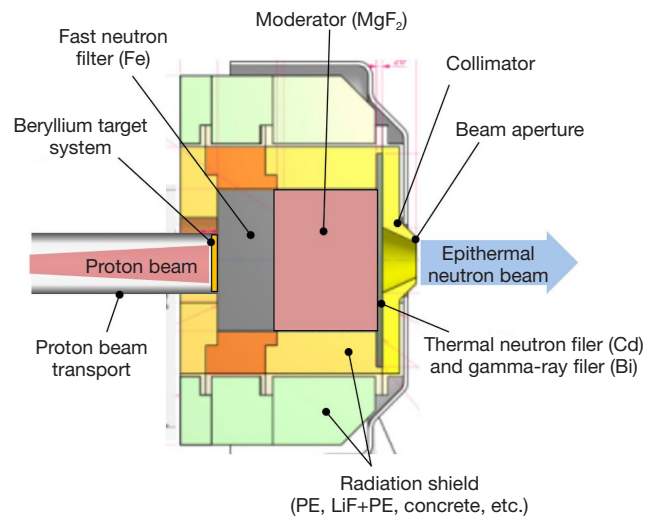


Figure 19 BSA of iBNCT (5). BSA, beam shaping assembly.

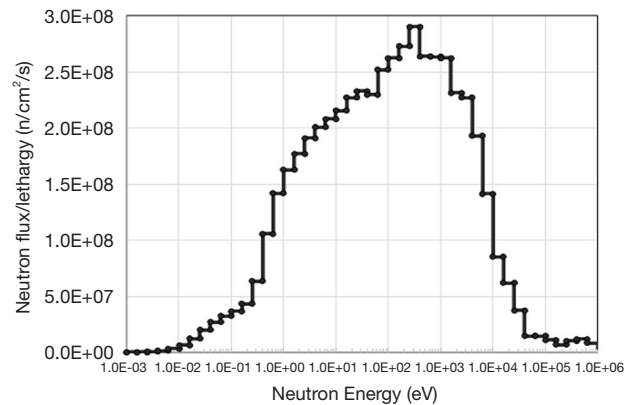


Figure 20 Energy spectrum at iBNCT BSA (5). BSA, beam shaping assembly.

moderator  $\text{CaF}_2$  is used. The energy spectrum of this system is shown in Figure 18 with a comparison of KUR facility (4). The energy spectra include higher energy component and the characteristics enable us to treat deeper position cancers. Similar system was built in two hospitals in Japan (6,7).

iBNCT was constructed in Tokai village in Ibaraki prefecture (5). The proton energy is 8 MeV and the current expected is 5 mA. The BSA is shown in Figure 19 (5). Main components of the BSA are Fe filter,  $\text{MgF}_2$  moderator and Pb reflector. The energy spectrum is shown in Figure 20. The spectrum of iBNCT has higher epithermal component compared with the reactor source, but fast neutron component is lower than that of C-BENS.

**Table 3** Radioactive products created by nuclear reactions in the moderator and iron filter

Material	RI	Reaction	Threshold E (MeV)
F	F-20	$^{19}\text{F}(n,\gamma)^{20}\text{F}$	–
	F-18	$^{19}\text{F}(n,2n)^{18}\text{F}$	11.0
	N-16	$^{19}\text{F}(n,\alpha)^{16}\text{N}$	3.0
Mg	Mg-27	$^{26}\text{Mg}(n,\gamma)^{27}\text{Mg}$	–
	Na-24	$^{24}\text{Mg}(n,p)^{24}\text{Na}$	5.3
Ca	Ca-49	$^{48}\text{Ca}(n,\gamma)^{49}\text{Ca}$	–
	Sc-49	$^{48}\text{Ca}(n,\gamma)^{49}\text{Ca}, (\beta^-) \rightarrow ^{49}\text{Sc}$	–
	Ar-37	$^{40}\text{Ca}(n,\alpha)^{37}\text{Ar}$	1.0
	Ca-45	$^{44}\text{Ca}(n,\gamma)^{45}\text{Ca}$	–
	Ca-47	$^{46}\text{Ca}(n,\gamma)^{47}\text{Ca}$	–
		$^{48}\text{Ca}(n,2n)^{47}\text{Ca}$	10
	K-42	$^{42}\text{Ca}(n,p)^{42}\text{K}$	3.6
	K-43	$^{43}\text{Ca}(n,p)^{43}\text{K}$	2.0
	Al	Al-28	$^{27}\text{Al}(n,\gamma)^{28}\text{Al}$
Mg-27		$^{27}\text{Al}(n,p)^{27}\text{Mg}$	2.5
Na-24		$^{27}\text{Al}(n,\alpha)^{24}\text{Na}$	5.4
Fe	Mn-56	$^{56}\text{Fe}(n,p)^{56}\text{Mn}$	4.5
	Fe-59	$^{58}\text{Fe}(n,\gamma)^{59}\text{Fe}$	–
	Fe-55	$^{54}\text{Fe}(n,\gamma)^{55}\text{Fe}$	–
	Mn-54	$^{54}\text{Fe}(n,p)^{54}\text{Mn}$	1.0

## Radioactivity

Low activation of the system is required for safer operation. The radioactivity at a time less than few hours after irradiation will be important for daily operation. Radioactive materials are produced by neutron reactions, and the products depend on the neutron energy, namely, the proton energy. *Table 3* shows radioactive products created in the moderator and Fe-filter, and *Table 4* shows decay characteristics of the radioactive nuclei.

F produces  $^{20}\text{F}$  with a half-life of 11.5 sec by neutron absorption and does not produce long half-life products less than 11 MeV.  $^{20}\text{F}$  is dominant just after the irradiation. When using a high energy proton over about 13 MeV,  $^{18}\text{F}$  with a half-life of 109.8 min is produced, and this remains at long time after the irradiation. Mg produces two nuclei  $^{27}\text{Mg}$  by neutron absorption and  $^{24}\text{Na}$  by (n, $\alpha$ ) reaction over 5.3 MeV. The former has a short half-life, 9.5 min, and the latter

**Table 4** Decay type, half-life and energy of emitted radiations of produced radioactive nuclei

RI	Decay type	Half life	Energy (MeV)
F-20	$\beta^-$	11.5 s	$\beta$ : 5.4, $\gamma$ : 1.63
F-18	$\beta^+$	109.8 m	$\beta^+$ : 1.66 (97) EC (3)
N-16	$\beta^-, \alpha$ (0.0006)	7.14 s	$\beta$ : 10.4, $\gamma$ : 7.11, 6.13 (69)
Mg-27	$\beta^-$	9.45 m	$\beta$ : 1.75, $\gamma$ : 0.40, 1.35 (70)
Na-24	$\beta^-$	15.0 h	$\beta$ : 1.39, $\gamma$ : 1.369, 2.754
Ca-49	$\beta^-$	8.8 m	$\beta$ : 1.95, $\gamma$ : 3.10 (89)
Sc-49	$\beta^-$	57 m	$\beta$ : 2.01, $\gamma$ : 1.76 (0.03)
Ar-37	EC	35.1 d	$\gamma$ : non
Ca-45	$\beta^-$	165 d	$\beta$ : 0.252, $\gamma$ : non
Ca-47	$\beta^-$	4.53 d	$\beta$ : 0.67, $\gamma$ : 1.3 (74), 0.8
K-42	$\beta^-$	12.4 h	$\beta$ : 3.52, $\gamma$ : 1.524 (18)
K-43	$\beta^-$	22.4 h	$\beta$ : 0.83, $\gamma$ : 0.62 (81)
Al-28	$\beta^-$	2.27 m	$\beta$ : 2.86, $\gamma$ : 1.78
Mn-56	$\beta^-$	2.57 h	$\beta$ : 2.85, $\gamma$ : 0.84 (99), 1.8
Fe-59	$\beta^-$	45.6 d	$\beta$ : 0.475, $\gamma$ : 1.29, 1.095
Fe-55	EC	2.60 y	$\gamma$ : non
Mn-54	EC	303 d	$\gamma$ : 0.835 (100), e: 0.83

Parentheses indicates percent of each radiation scheme.

15.0 hours.  $^{24}\text{Na}$  is major nucleus of residual radioactivity in the case of  $\text{MgF}_2$  moderator, but the nucleus is produced by neutrons with energy above 5.3 MeV. Therefore,  $^{24}\text{Na}$  contribution will be small at proton energy lower than about 8 MeV.  $^{49}\text{Ca}$  emitted  $\gamma$ -rays and the half-life is 8.8 m. Therefore, this nucleus is dominant in a short period after the irradiation.  $^{37}\text{Ar}$  radiation become dominant at longer time but this nucleus emits a very low energy characteristic X-ray with an energy of 2.58 keV as a product of the decay of  $^{49}\text{Ca}$ , and it will be very easily shielded. In the case of Al, radioactivity comes from  $^{28}\text{Al}$  by neutron absorption,  $^{27}\text{Mg}$  by (n,p) with a threshold energy of 2.5 MeV and  $^{24}\text{Na}$  by (n, $\alpha$ ) with a threshold energy of 5.4 MeV.  $^{28}\text{Al}$  has a short half-life of 2.27 m and become negligible after few ten minutes. The contributions of  $^{27}\text{Mg}$  and  $^{24}\text{Na}$  depend on proton energy and  $^{24}\text{Na}$  radioactivity exist at rather long time after irradiation due to 15.0 hours half-life. In the case of Fe, four radioactive materials are produced.  $^{55}\text{Fe}$  and  $^{59}\text{Fe}$  are created by neutron absorption, and  $^{54}\text{Mn}$  and  $^{56}\text{Mn}$  by (n,p) reaction, in which threshold energies are 1.0 MeV and 4.5

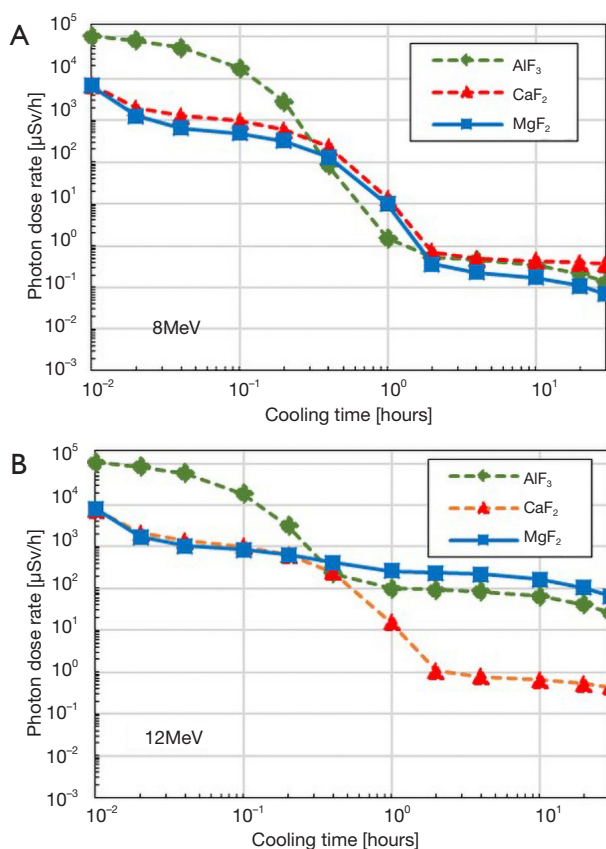


**Figure 21** Dose around the exit of the BSA for different moderator materials at 8 MeV (A) and 12 MeV (B). Fe-filter data are also indicated (34). BSA, beam shaping assembly.

MeV, respectively.  $^{56}\text{Mn}$  has a half-life of 2.57 hours. On the other hand,  $^{54}\text{Mn}$  has a half-life of 303 days. Therefore,  $^{56}\text{Mn}$  will be a main contributor in a period of few hours after irradiation.

From the quantitative consideration written above, it is expected that the residual activity depends on the moderator material and the proton energy. Figure 21 shows dose data around the exit of the collimator under the condition that each system gives the same epithermal neutron intensity with the same fast neutron component at each proton energy (34). Figure 21A is the data at 8 MeV and Figure 21B at 12 MeV. At 8 MeV, for  $\text{MgF}_2$  and  $\text{CaF}_2$  BSA cases the effect of  $^{20}\text{F}$  is observed at early time and then  $^{27}\text{Mg}$  and  $^{49}\text{Ca}$  become dominant in the total dose and the decays of both nuclei are almost the same since they have almost the same half-life. After them, dose from  $^{24}\text{Na}$  appears in the case of Mg and  $^{37}\text{Ar}$  in the case of Ca. In the case of  $\text{AlF}_3$ ,  $^{28}\text{Al}$  is dominant at the early time and then  $^{24}\text{Na}$ . At 12 MeV

contribution of  $^{24}\text{Na}$  become larger at a time later than about 1 hour both in Mg and Al case. On the other hand, the dose of the Ca case is almost the same between 8 and 12 MeV since the same neutron reactions contributes to the dose. Therefore, at the proton energy larger than about 10 MeV  $\text{CaF}_2$  will be better and at the energy lower than this energy  $\text{MgF}_2$  will be better.

## Summary

Consideration on the BSA design based on the IAEA TECDOC-1223 was presented. Some of the quantitative values may change depending on the further optimization of the BSA. A thermal neutron source for cancers at a shallow position should be considered although it was not discussed in detail in this paper. If considering the dismantlement of the facility, long lived radioisotopes should be also evaluated such as T produced by Li, Po by Bi etc.

## Acknowledgments

The author sincerely thanks Drs. Y. Sakurai, H. Kumada, H. Tanaka and F. Hiraga for supplying valuable data, and also Ms. Y. Hashimoto, Mr. A. Sato and Mr. R. Inoue since many useful results were referred from their master theses.

*Funding:* None.

## Footnote

*Provenance and Peer Review:* This article was commissioned by the Guest Editors (Hiroaki Kumada and Yi-Wei Chen) for the series “Boron Neutron Capture Therapy” published in *Therapeutic Radiology and Oncology*. The article has undergone external peer review.

*Conflicts of Interest:* The author has completed the ICMJE uniform disclosure form (available at <http://dx.doi.org/10.21037/tro.2018.10.05>). The series “Boron Neutron Capture Therapy” was commissioned by the editorial office without any funding or sponsorship. The author has no other conflicts of interest to declare.

*Ethical Statement:* The author is accountable for all aspects of the work in ensuring that questions related to the accuracy or integrity of any part of the work are appropriately investigated and resolved.

*Open Access Statement:* This is an Open Access article

distributed in accordance with the Creative Commons Attribution-NonCommercial-NoDerivs 4.0 International License (CC BY-NC-ND 4.0), which permits the non-commercial replication and distribution of the article with the strict proviso that no changes or edits are made and the original work is properly cited (including links to both the formal publication through the relevant DOI and the license). See: <https://creativecommons.org/licenses/by-nc-nd/4.0/>.

## References

- Bavarnegin E, Kasesaza Y, Wagner FM. Neutron beams implemented at nuclear research reactors for BNCT. *J Instrumentation* 2017. doi: 10.1088/1748-0221/12/05/P05005.
- Ke G, Sun Z, Shen F, Liu, et al. The study of physics and thermal characteristics for in-hospital neutron irradiator (IHNI). *Appl Radiat Isot* 2009;67:S234-7.
- Anderson IS, Andreani C, Carpenter JM, et al. Research opportunities with compact accelerator-driven neutron sources, *Phys Report* 2016;654:1-58.
- Tanaka H, Sakurai Y, Suzuki M, et al. Measurement of the Thermal Neutron Distribution in a Water Phantom Using a Cyclotron Based Neutron Source for Boron Neutron Capture Therapy. *IEEE Nuclear Science Symposium Conference Record* 2009, Article number 5402230, Pages 2355-2357.
- Kumada H, Naito F, Hasegawa K, et al. Development of LINAC-Based Neutron Source for Boron Neutron Capture Therapy in University of Tsukuba. *Plasma and Fusion Research: Regular Articles* 2018;13:2406006.
- Southern Tohoku Hospital. Available online: <https://southerntohokubnct.com/>
- Osaka Medical College. Available online: <https://www.osakamed.ac.jp/kbmc/>
- National Cancer Center. Available online: [https://www.ncc.go.jp/jp/ncch/clinic/radiation\\_oncology/bnct/index.html/](https://www.ncc.go.jp/jp/ncch/clinic/radiation_oncology/bnct/index.html/)
- Durisi E, Alikaniotis E, Borla O, et al. Design and simulation of an optimized e-linac based neutron source for BNCT research. *Appl Radiat Isot* 2015;106:63-7.
- IAEA-TECDOC-1223: Current states of neutron capture therapy (IAEA 2001).
- Hawkesworth MR. Neutron radiography equipment and methods. *Atomic Energy Review* 1977;15:169-220.
- Cartelli D, Capoulat ME, Bergueiro J, et al. Present status of accelerator-based BNCT: Focus on developments, in Argentina. *Appl Radiat Isot* 2015;106:18-21.
- Lee CL, Zhou XL, Kudchadker RJ, et al. A Monte Carlo dosimetry-based evaluation of the  ${}^7\text{Li}(p,n){}^7\text{Be}$  reaction near threshold for accelerator boron neutron capture therapy. *Med Phys* 2000;27:192-202.
- Waters LS, McKinney GW, Durkee JW, et al. The MCNPX Monte Carlo Radiation Transport Code. *AIP Conference Proceedings* 2007;896:81-90.
- Shibata K, Iwamoto O, Nakagawa T, et al. JENDL-4.0: A New Library for Nuclear Science and Engineering. *J Nucl Sci Technol* 2011;48:1-30.
- Fujimoto N, Tanaka H, Sakurai Y, et al. Improvement of depth dose distribution using multiple-field irradiation in boron neutron capture therapy. *Appl Radiat Isot* 2015;106:134-8.
- Astrelin VT, Burdakov AV, Bykov PV, et al. Blistering of the selected materials irradiated by intense 200 keV proton beam. *J Nucl Mat* 2010;396:43-8.
- Nishimura C, Komaki M, Amano M. Hydrogen permeation characteristics of vanadium-nickel alloys. *Mater Trans* 1991;32:501-7.
- Bauer HC, Völkl J, Tretkowski J, et al. Diffusion of hydrogen and deuterium in Nb and Ta at high concentrations. *Z Phys B* 1978;29:17-26.
- Wipf H. Solubility and diffusion of hydrogen in pure metals and alloys. *Phys Scr* 2001;T94:43-51.
- Ishikawa T, Mclellan RB. The diffusivity of hydrogen in copper at low temperature. *J Phys Chem Solids* 1985;46:445-7.
- Yamagata Y, Hirota K, Ju J, et al. Development of a neutron generating target for compact neutron sources using low energy proton beams. *J Radioanal Nucl Chem* 2015;305:787-94.
- Kurihara Y, Kobayashi H, Matsumoto H, et al. Neutron target research and development for BNCT: direct observation of proton induced blistering using light-polarization and reflectivity changes. *J Radioanal Nucl Chem* 2015;305:935-42.
- Yano S, Tada M, Matsui H. Hydrogen embrittlement of MFR candidate vanadium alloys. *J Nucl Mater* 1991;179-181:779-82.
- Nambu T, Shimizu K, Matsumoto Y, et al. Enhanced hydrogen embrittlement of Pd-coated niobium metal membrane detected by in situ small punch test under hydrogen permeation. *J Alloy Compd* 2007;446-447:588-92.
- Kumada H, Kurihara T, Yoshioka M. et al. Development of beryllium-based neutron target system with three-layer structure for accelerator-based neutron source for boron

- neutron capture therapy. *Appl Radiat Isot* 2015;106:78-83.
27. Halfon S, Arenshtama A, Kijel D, et al. Demonstration of a high-intensity neutron source based on a liquid-lithium target for Accelerator based Boron Neutron Capture Therapy. *Appl Radiat Isot* 2015;106:57-62.
  28. Horiike H, Murata I, Iida T, et al. Liquid Li based neutron source for BNCT and science application, *Appl Radiat Isot* 2015;106:92-94.
  29. Nakamura S, Imamich S, Masumoto K, et al. Evaluation of radioactivity in the bodies of mice induced by neutron exposure from an epithermal neutron source of an accelerator-based boron neutron capture therapy system. *Proc Jpn Acad* 2017;Ser. B 93:821-31.
  30. Helsinki University Hospital. Available online: <http://www.hus.fi/hus-tietoa/uutishuone/Sivut/BNCT-sädehoitolaite-HUSiin-ensimmäisenä-maailmassa.aspxospital>
  31. Uritani A, Menjo Y, Watanabe K, et al. Design of Beam Shaping Assembly for an Accelerator-driven BNCT System in Nagoya University. *JPS Conf Proc* 2018;22:011002.
  32. Sato T, Iwamoto Y, Hashimoto S, et al. Features of Particle and Heavy Ion Transport code System (PHITS) version 3.02. *J Nucl Sci Technol* 2018;55:684-90.
  33. Inoue R, Hiraga F, Kiyonagi Y. Optimum design of a moderator system based on dose calculation for an accelerator driven Boron Neutron Capture Therapy. *Appl Radiat Isot* 2014;88:225-8.
  34. Hashimoto Y, Hiraga F, Kiyonagi Y. Optimal moderator materials at various proton energies considering photon dose rate after irradiation for an accelerator-driven  $^9\text{Be}(p, n)$  boron neutron capture therapy neutron source. *Appl Radiat Isot* 2016;106:88-91.
  35. Sakurai Y, Kobayashi T. Spectrum evaluation at the filter-modified neutron irradiation field for neutron capture therapy in Kyoto University Research Reactor. *Nucl Instr Meth Phys Res* 2004;A531:585-95.

doi: 10.21037/tro.2018.10.05

**Cite this article as:** Kiyonagi Y. Accelerator-based neutron source for boron neutron capture therapy. *Ther Radiol Oncol* 2018;2:55.